

Document downloaded from:

<http://hdl.handle.net/10251/202185>

This paper must be cited as:

Patrao Herrero, I.; González-Medina, R.; Garcerá, G.; Figueres Amorós, E. (2023). An Algorithm for Emulating Photovoltaic Strings With Dynamic Partial Shadowing Capability: A Practical Study. IEEE Industrial Electronics Magazine. 17(2):61-69.
<https://doi.org/10.1109/MIE.2022.3151017>



The final publication is available at

<https://doi.org/10.1109/MIE.2022.3151017>

Copyright Institute of Electrical and Electronics Engineers

Additional Information

An algorithm for emulating photovoltaic strings with dynamic partial shadowing capability

In photovoltaic (PV) systems, a maximum power point tracking (MPPT) algorithm is needed to maximize the energy obtained from the PV strings [1, 2]. A bad tracking of the maximum power point (MPP) degrades the overall performance of the photovoltaic facilities [3-6]. The panels in a PV string may be working under different operating conditions of irradiance and temperature because of eventual shades produced by near obstacles, different orientation of modules or dusting, resulting in the partial shadowing phenomenon [7, 8].

PV panels could be used to test MPPT algorithms. However, reproducing the desired weather conditions in a controlled and repeatable way is not an easy task. To take control of the testing conditions in laboratories, commercial PV emulators are usually used instead of PV panels, but they present some limitations, particularly in fast irradiance transitions and, more often, when emulating long periods of time (for instance, 1 day). A detailed analysis of such limitations was listed in [9]. Some of the PV emulators commercially available store the model of a single PV string I-V curve at fixed irradiance and temperature conditions and cannot reproduce a variation of these parameters over the time [10-14]. Modern PV emulators provide dynamic partial shadowing emulation, but their high cost hinders their application in educational or professional training environments [15] and in research laboratories with the presence of a huge amount of PV power converters to be tested at the same time, like microgrid test beds. In such cases, the acquisition of many expensive PV emulators with dynamic partial shadowing capability may be unaffordable. An emulator of a few kilowatts of power is usually over thousands of euros, while the cost of the emulator proposed by the authors is around 200€.

In this paper a low computational cost algorithm for emulating PV strings with dynamic partial shadowing capability is presented, suitable for microcontroller-based emulators. It is based on the emulator proposed in [16]. The developed algorithm rebuilds the I-V curve of the whole string on-the-fly, according to an irradiance and temperature time-varying profile for each panel.

In order to demonstrate the performance of the proposed algorithm, a PV string consisting of 14 series-connected PV panels feeding a single-phase grid connected inverter (230 V, 50 Hz) has been emulated under time-varying irradiance and partial shadowing conditions in section “Experimental Results”.

PHOTOVOLTAIC MODULE AND PARTIAL SHADOWING

A. PV panel model

A PV panel presents a characteristic current-voltage (I-V) curve which mathematical models and equivalent circuits that have been widely studied in the literature [17, 18]. The mathematical model of an ideal PV cell can be represented by means of equations (1) and (2). (T) is the temperature in Kelvin degrees and (ΔT) is the increment of temperature from the nominal value. (V) is the output voltage and (I) is the output current. (I_0) is the dark current and (I_L) is the light generated current. (G) is the sun irradiance. ($I_{L,n}$) and (G_n) are the light generated current and the sun irradiance at nominal test values, respectively. The Boltzmann constant is represented by (k), (q) is the electron charge, (a) is the ideality diode constant and (n) is the number of PV panels.

$$I = I_L - I_0 \left(e^{\left(\frac{q \cdot V}{N_s \cdot k \cdot T \cdot a} \right)} - 1 \right) \quad (1)$$

$$I_L = (I_{L,n} + K_I \cdot \Delta T) \cdot \frac{G}{G_n} \quad (2)$$

Manufacturers usually provide PV panel specifications and two set of experimental I-V curves at standard test conditions (STC, 25°C and 1000W/m²). These curves show an irradiance sweep obtained at 25°C and a temperature sweep at 1000W/m². Manufacturers also provide temperature coefficients for short circuit current and open circuit voltage. Although the theoretical model parameters can be obtained from the experimental data curve at STC, a lookup table from the I-V curve has been used as input data for the emulator. In the following, the dependence of the panel parameters on the irradiance and temperature will be studied. From the open-circuit voltage and the short-circuit current behaviour, the data in the look-up table are adapted to any irradiance and temperature conditions.

B. Irradiance variations

It is convenient to avoid the use of the logarithmic or exponential calculations present in (3) and (6) for the generation of the curve, because their high computational cost. Polynomial operations are preferred instead, because of the characteristics of DSCs, which are optimized to perform fast multiply and accumulate mathematical operations.

According to (3), the light generated current (I_L) is proportional to the irradiance at 25°C [17-19]. Thus, by using the model in (1), it is possible to obtain the short-circuit current following (4). Note that the short circuit current can be obtained from (4) if the output voltage is zero ($V=0$), being the short-circuit current (I_{sc}) proportional to the irradiance value (G). An analogous irradiance-current behaviour can be applied to the original I-V curve, according to (5). Thus, the modified current data values are stored in an array, named Working Array (WA).

$$I_L(G, \Delta T) = \frac{G}{G_n} (I_{L,n} + K_I \cdot \Delta T) \xrightarrow{\Delta T=0} I_{pv}(G) = \frac{G}{G_n} I_{L,n} \quad (3)$$

$$I_{SC} = \frac{G}{G_n} I_{pv,n} - I_0 \left(e^{\left(\frac{q \cdot V}{N_s \cdot k \cdot T \cdot a} \right)} - 1 \right) \Big|_{V=0} = \frac{G}{G_n} I_{L,n} \quad (4)$$

$$I_{out,WA}(G) = \frac{G}{G_n} I_{out(STC)} \quad (5)$$

Equation (6) is obtained from (1) at nominal temperature (25°C). The open circuit voltage (V_{OC}) can be calculated from (6) if the output current is zero (7). As the use of polynomials is preferred over logarithmic functions, (7) is approximated by a second-degree polynomial equation (8), whose constant values (a, b, c) are obtained using the data from the original I-V curves provided by the manufacturer. Thus, an analogous irradiance—voltage behaviour can be applied to the original I-V curve according to (8). The modified voltage data values are stored in the WA.

$$V = \frac{N_s \cdot k \cdot T \cdot a}{q} \cdot \ln \left(1 + \frac{1}{I_0} \cdot \left(I - \frac{G}{G_n} \cdot I_{L,n} \right) \right) \quad (6)$$

$$V_{OC}(G) = V|_{I=0} = \frac{N_s \cdot k \cdot T \cdot a}{q} \cdot \ln \left(1 - \frac{G}{G_n} \cdot \frac{I_{L,n}}{I_0} \right) \quad (7)$$

$$V_{out,WA}(G) = (a \cdot G^2 + b \cdot G + c) \cdot V_{out(STC)} \quad (8)$$

C. Temperature variations

The effect of temperature variations has been described in [17, 18]. Manufacturers provide the I-V curves and the temperature coefficients of V_{OC} (K_V), I_{SC} (K_I) and power as a % variation per degree around the nominal values. Two linear modifications for considering temperature variations are imposed to the voltage and current data, following (10) and (11), respectively. The new I-V curve data, I_{out,WA}(T) and V_{out,WA}(T), are overwritten to the WA updating the previous values, I_{out,WA} and V_{out,WA}, which have been calculated at nominal temperature.

$$I_{out,WA}(T) = (T - T_{nom}) \cdot K_I + I_{out,WA} \quad (10)$$

$$V_{out,WA}(T) = (T - T_{nom}) \cdot K_V + V_{out,WA} \quad (11)$$

D. PV string model and partial shadowing

The output voltage of a PV string is the sum of the voltages of each panel for a given string current; therefore, performing a sweep of the string current provides the I-V curve of a PV string. The operating point of each panel is linked to the other panels since the current of all of them is the same.

If all the PV panels of the string are operating under the same irradiance and temperature conditions, the resultant I-V curve of the string is equivalent to that of a single panel, but the output voltage is multiplied by the number of panels. If the panels are operating under different conditions, the phenomenon of partial shadowing appears, because the I-V curve of each panel is different.

A PV string curve under partial shadowing presents various local MPPs and one global MPP [20, 21]. The presence of various MPPs complicates the correct operation of traditional MPPTs algorithms, like the Perturb&Observe one (P&O) [7, 8], reducing the efficiency of the PV system. The objective of any MPPT algorithm is to find the MPP in the string P-V curve and keep it working at this operation point. The global MPP of the whole string must be reached rather than any of the local MPPs of individual panels. Therefore, the study of advanced techniques for MPPT algorithms and their effectiveness is of great importance in PV facilities [22-24].

PHOTOVOLTAIC EMULATOR

A. Power Converter

The PV source emulator is based on the 3 kW PV emulator presented in [16]. The power stage is a buck DC-DC converter working with average current mode control [17], being operated as a controlled current source in which the output current reference depends on the output voltage. The I-V relationship follows the I-V curve of the emulated PV string.

That curve is generated by an embedded digital signal controller (DSC) according to the PV source model, the irradiance level and the programmed temperature. The schematic diagram of the DC/DC converter is shown in figure 1. The emulator is powered by an external DC power supply of 550V. The terminals which behave as PV panels (V_{OUT}) are connected directly to the input of the PV inverter under test. The string configuration and the irradiance and temperature profiles are programmed in the microcontroller. The transient in the irradiance profile is triggered by an external source.

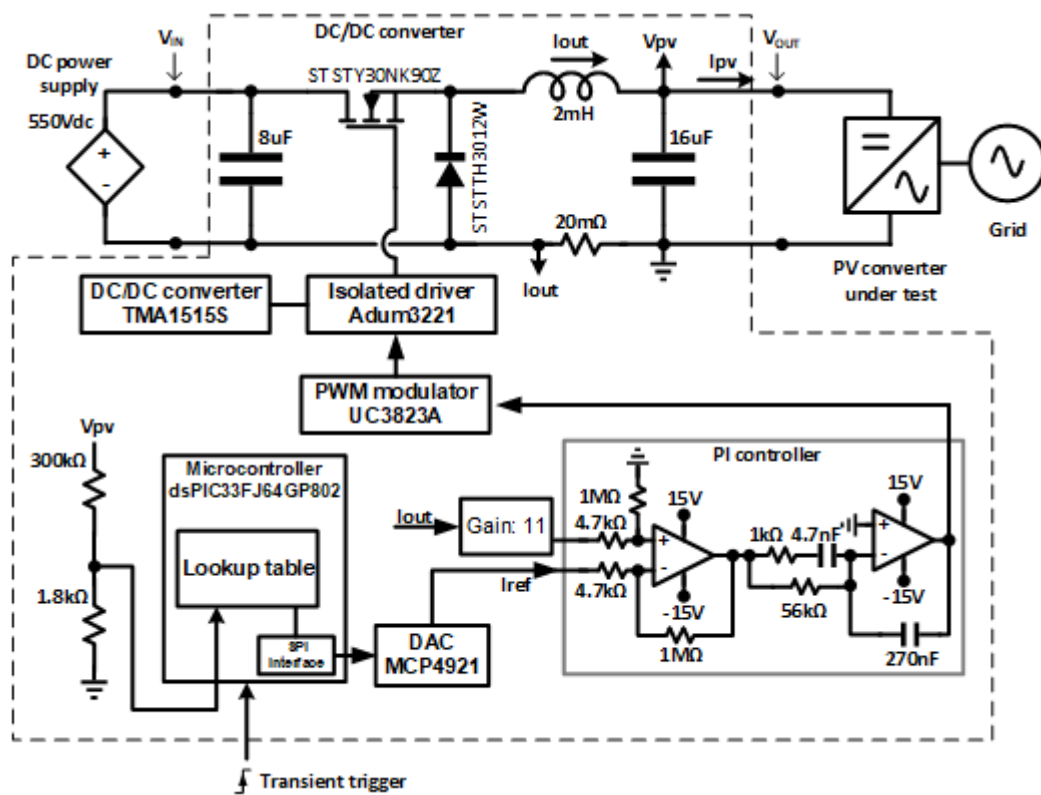


Fig1. PV emulator DC/DC converter.

This control scheme avoids an output voltage control loop in the DC-DC converter. The lack of output voltage control of the DC-DC converter allows the connection to PV inverters, which are usually provided with a large input DC-Link capacitor bank and a DC-Link voltage controller. Note that the input voltage of the inverter agrees with the output voltage of the DC-DC converter. The dynamic behaviour of the DC-DC converter

which emulates the PV string (with a crossover frequency of the current loop around 10kHz) is fast enough for testing PV inverters. The string V/I curve is updated every 200ms, fast enough for testing most climate transitions, even a 1-day irradiation profile for energy harvesting tests.

The selected DSC for this application is the Microchip dsPIC33FJ128GP802 (16bits, 40MIPS). The algorithm is optimized to perform most math operations in 16-bit integer variables. The algorithm which processes the I-V data provided by the PV module manufacturer has been optimized for its fast execution on a low-cost DSC, performing one clock-cycle duration multiply-and-accumulation operations instead of time consuming logarithmic or exponential calculations. The microcontroller has an internal 12-bit ADC, which is used to acquire the output voltage. A 12-bit DAC is connected to the Seral Port Interface (SPI) port of the microcontroller to provide an analog reference for the average output current control.

Two software execution threads are programmed, namely the background and the real-time execution threads. The background thread updates the PV string model according to irradiance and temperature time-varying profiles programmed by the user. The real-time thread running in the foreground updates the DC-DC converter current reference at 1 kHz.

B. Generation of the I-V curve at the desired irradiance and temperature working conditions

The generation of the I-V curve for each PV panel at the desired working operating conditions of irradiance and temperature is calculated on-the-fly from the original I-V curve, which is provided at nominal working conditions (1000W/m² and 25°C). The original I-V curve data are stored into an array (original array, OA) which contains 26 pairs of I-V points. It is a good practice entering most of the points of the original array

near the MPP to achieve greater accuracy at this point, since a linear interpolation is used. The data of the OA are sorted in ascending order of voltage values. The voltage and current digital data are treated in the DSC as 16 bit integer values. Because of the 12 bit DAC and ADC, the digital range starts from zero, reaching the full scale at 4095. The analog current full scale is 10 A and the voltage full scale is 40 V for a single panel. The PV string voltage full scale is 560 V. Original I-V curve values are entered in the OA according to their equivalent digital values.

C. Extended working array (EWA)

Linear interpolation is used for the string I-V generation because of the low computational cost required. In each interpolation the difference between adjacent points is required. To improve the interpolation speed, the voltage and current increment between two adjacent points in the I-V original curve is precalculated. These data are stored adding two rows to the WA, thus creating the Extended Working Array (EWA). The size of the EWA is 4x26.

D. Generation of a PV array made of 14 series-connected panels

The emulated PV string is made of panels with an MPP voltage of 29 V_{DC} and an MPP power of 230 W each at standard test conditions (STC). A string of 14 panels connected in series provides enough voltage (406 V_{DC}) for injecting a power around 3220 W to a 230 V_{RMS} single-phase grid using a single-stage PV inverter. To balance the computational cost of the algorithm with the update rate of the I-V curve of the whole string, the time-varying profiles of irradiance and temperature are limited to 7. Therefore, the emulated string has 7 blocks of two panels connected in series. As a result, the features of 14 series connected PV panels can be modelled, but only 7 time-varying profiles of irradiance and temperature are executed. The proposed solution is realistic enough and avoids the need of an expensive DSC. It's worth pointing out that the number

of 14 panels comes from the input voltage usually used in single-stage single-phase inverters connected to a 230 V_{RMS} grid. The proposed algorithm has no theoretical limit in the number of series-connected modules. However, the electronic components used in the DC-DC converter stage are limited to 600 V, so that only 14 PV panels can be emulated.

Each PV panel in the string must have its own I-V curve as the working conditions of each one may differ. Therefore, 14 I-V panel curves must be generated applying irradiance and temperature variations to the original curve. These panel curves are stored in the string panels array (SPA).

Working conditions changes in real time, so that these curves are continuously updated by the background thread. The 14 panels are grouped in blocks of two to reduce the memory requirements and the computation time for generating all I-V curves. Thus, 7 curves are calculated and stored in the SPA which has a size of 7xEWA (7x[4x26]).

E. String generation

The string I-V curve is built from the data in the SPA, which contains the I-V curves of the panels in the string at their working conditions. The output voltage of the string is the sum of the voltage of each panel for a given current.

The string generation algorithm has been programmed to obtain the string I-V curve. It performs a decreasing current sweep from the full scale of current (10A) to zero. The data are treated as their equivalent digital values. Therefore, the sweep starts on a current value of 4094 (rounded from 4095) and ends at the value of zero, in decremental steps of 2. As a result, a vector of 2048 elements is obtained in which the index of each element corresponds to a current value. This vector is used as the string look-up table (SLT) which provides the DC-DC converter output current reference for a sensed output voltage. Due

to the sweep in steps of 2, the digital value of the current of each element is twice of its index value.

The value of each element corresponds to the sum of the voltages of all the PV panels in the string at a current value equal to twice of its index. Since the full scale of the PV panels is $40V=4095$, the digital full scale of the sum of 14 panels is $4095 \times 14 = 57330$. This value is scaled in the algorithm ($1/14$) to meet the string full scale, $560V=4095$, and stored in the corresponding item of the SLT.

This algorithm is executed 2048 times per curve update. It performs 7×2048 linear interpolations. Each interpolation needs the voltage and current increment between two adjacent points in the I-V curve. The generation of the EWA instead of the WA adds $26 \times 2 \times 7 = 364$ operations per curve, saving $2048 \times 2 \times 7 = 28672$ operations in the interpolation. It is a reduction of 28308 mathematical operations which allows a faster refresh of the string curve. The generation of the SPA and the SLT is processed in the background continuously. The generation of each SLT is completed in approximately 200 ms. The whole algorithm that generates the SPA and the SLT is shown in figure 2.

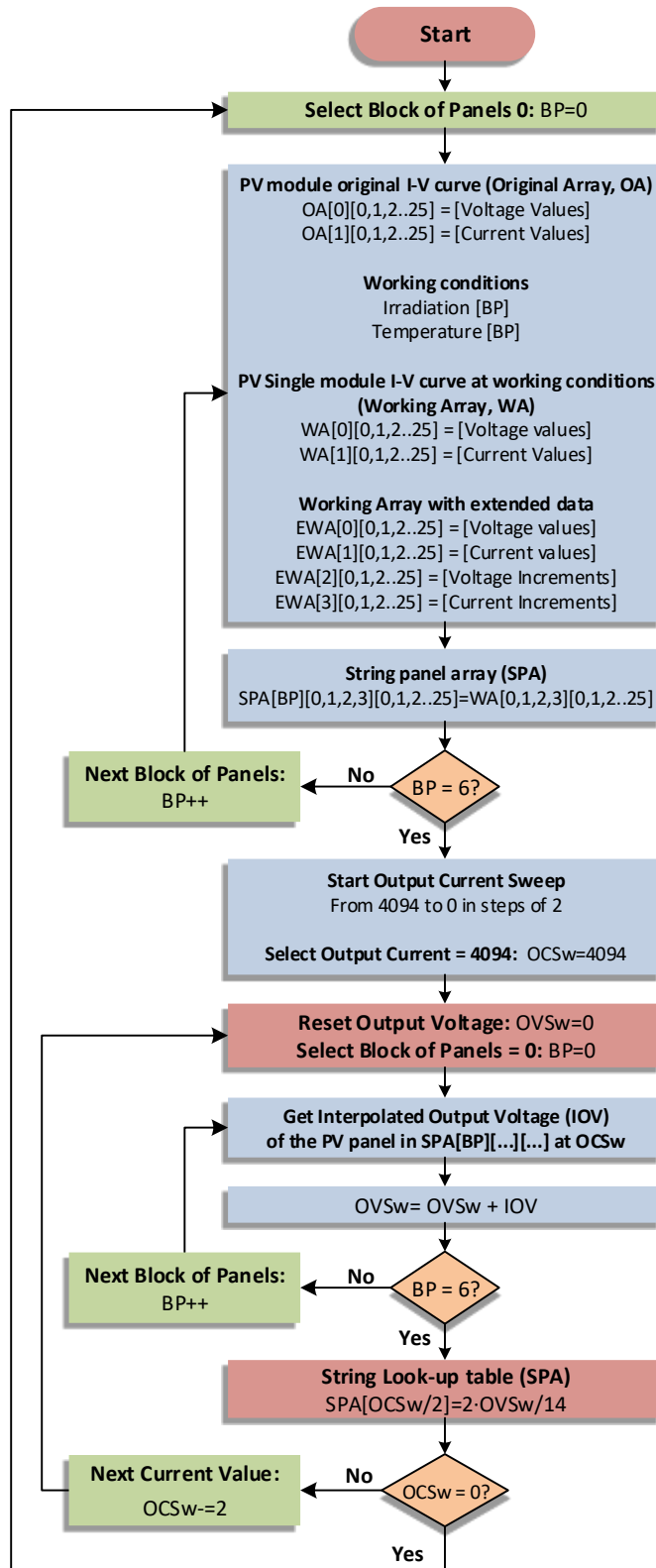


Fig. 2. PV string generation algorithm chart flow

F. Generation of the reference current for the DC-DC converter

The real-time processing algorithm runs in the foreground thread managed by the ADC

interrupt (1 kHz). Each time the interrupt is launched the internal ADC acquires the output voltage. The search algorithm is executed to find the DC-DC converter current reference in the SLT, being this reference updated at the DAC. The flowchart of the reference current generation algorithm is represented in figure 3.

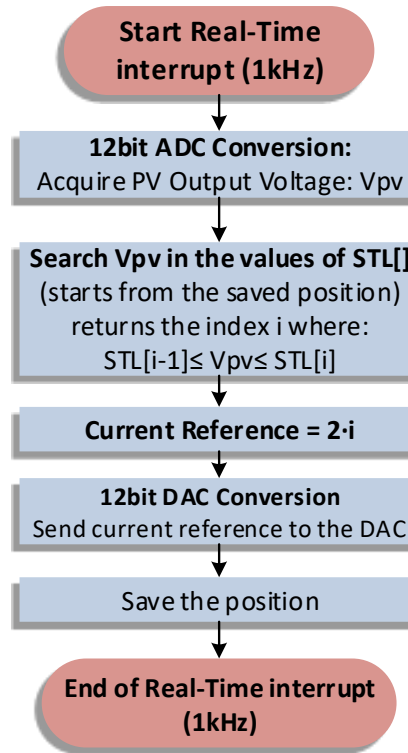


Fig. 3. Current reference generation algorithm flowchart

The digital value of the output voltage is used as an input value for the search algorithm. The algorithm searches in the SLT the interval in which the output voltage is found. The index of the item that corresponds to the upper value of the interval is used as half of the current reference value. Therefore, the value loaded into the DAC is this index multiplied by 2.

The search algorithm uses the following technique: the search starts in the previous selected item of the SLT (the selected item at the boot is zero). If the present voltage is equal than the previous, the new selected value is the same. If the present voltage value

is lower than the previous, the search continues in ascending order of the items. If the voltage value is higher, the process continues in descending order.

G. Calculus on-the-fly

Using two threads with different priority enables the emulator to show a fast dynamic performance to test MPPT algorithms with a high refresh frequency (1 kHz), changing the string I-V curve according to time-varying working conditions profiles.

EXPERIMENTAL RESULTS

In the first set of tests (called A, B, and C), the emulator has been fed by an AMREL SPS800-12 DC power supply. A Chroma 63803 programmable DC-Load performs voltage sweeps under different irradiance and temperature conditions from the open-circuit voltage of the string to the minimum voltage permitted by the DC-Load.

In the last test (D), the output of the emulator was connected to a single-stage grid-connected voltage source inverter (VSI) which controls the voltage of the DC-Link. To perform MPPT tests, the inverter injects power to a single-phase 230 V_{RMS} and 50 Hz grid. The minimum DC-Link voltage reference of the VSI MPPT algorithm has been set to 380 V, in order to properly work connected to the grid.

A. Current reference generation and I-V curve generation tests without partial shadows

The objective of this experiment is to compare the static curves provided by the manufacturer and the I-V curves measured at the output of the emulator. The comparison is made for different levels of irradiance and temperature.

All the panels in the string are configured at the same irradiance and temperature, remaining unchanged during each sweep.

A set of five sweeps is performed at 25°C and irradiances of 200, 400, 600, 800 and 1000W/m². The measured data (green dots) are plotted over the I-V curves provided by the manufacturer (red lines) in figure 4.

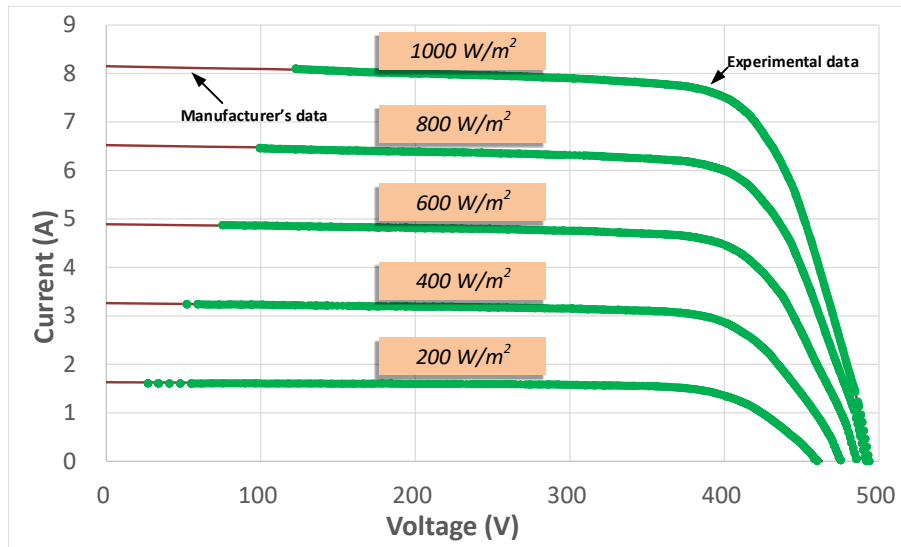


Fig. 4. Curve generation test for irradiance variations. Experimental data (green dots) over manufacturer's data (red lines). Temperature = 25°C.

A set of three sweeps has been performed at 1000W/m² and different temperatures. The measured data is plotted over the I-V curves provided by the manufacturer in figure 5.

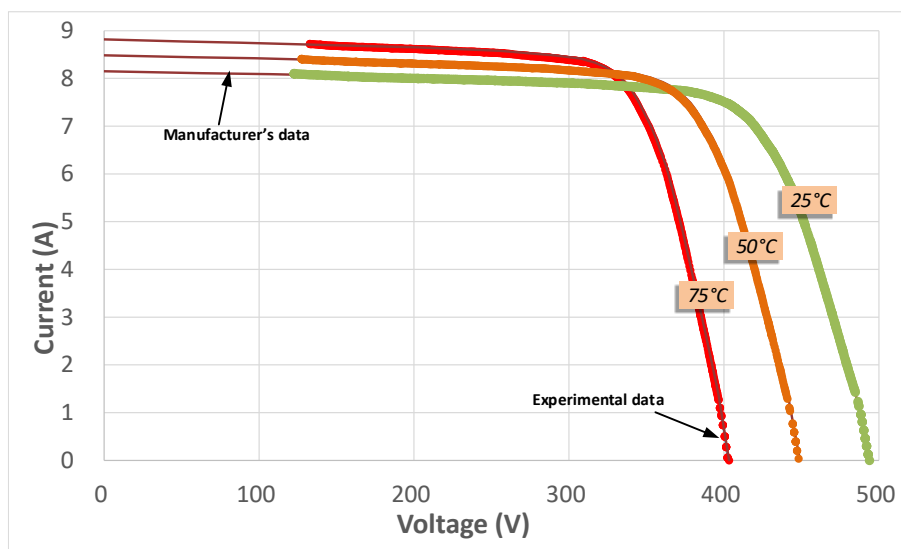


Fig. 5. Curve generation test for temperature variations. Experimental data (dots) over manufacturer's data (lines). Irradiation: $1000\text{W}/\text{m}^2$.

In the results it is observed that the experimental data accurately fit the manufacturer's PV panel curves.

B. Static I-V generation tests with partial shadows

To test the emulation of partial shadows, the working conditions configured for generating the string I-V curve are not the same for all panels. Figure 6 shows a multiple MPPs P-V curve for an irradiance set-up of 4 modules@ $800\text{W}/\text{m}^2$ + 4 modules@ $700\text{W}/\text{m}^2$ + 4 modules@ $600\text{W}/\text{m}^2$ + 2 modules@ $500\text{W}/\text{m}^2$ and 25°C .

The accuracy of the generated I-V curve is better than the 1% for most of the output voltage range. The relative error for the output current is depicted in figure 7. The error increases near the open-circuit voltage due to the higher slope of the I-V curve.

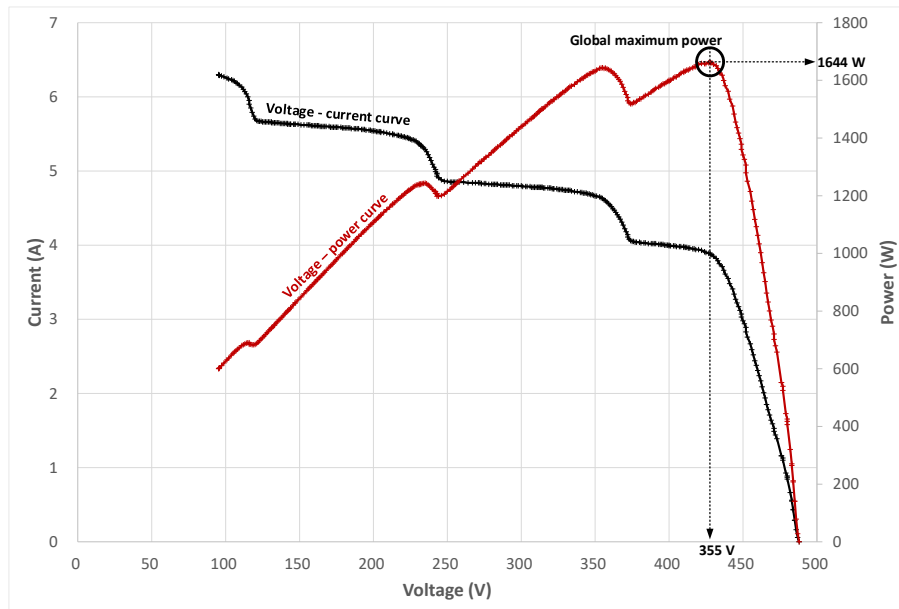


Fig. 6. I-V (black) and P-V (red) curves of the generated string curve with partial shadows. Temperature = 25°C .

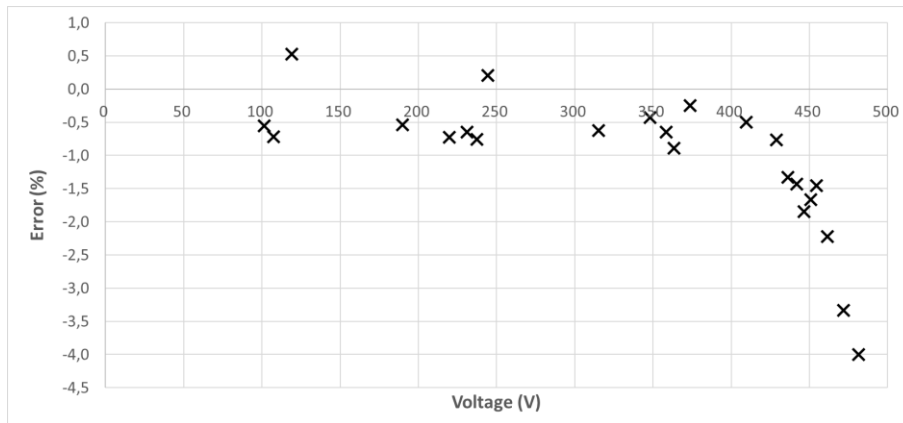


Fig. 7. Deviation in % error of the generated I-V values from the manufacturer's data

C. Dynamic I-V string curve generation tests with partial shadows and time-varying conditions

In this test the PV emulator feeds the PV grid-connected single-stage single-phase PV inverter, with the objective of testing the behaviour of the emulator under realistic time-varying conditions. The experimental setup is depicted in figure 8.

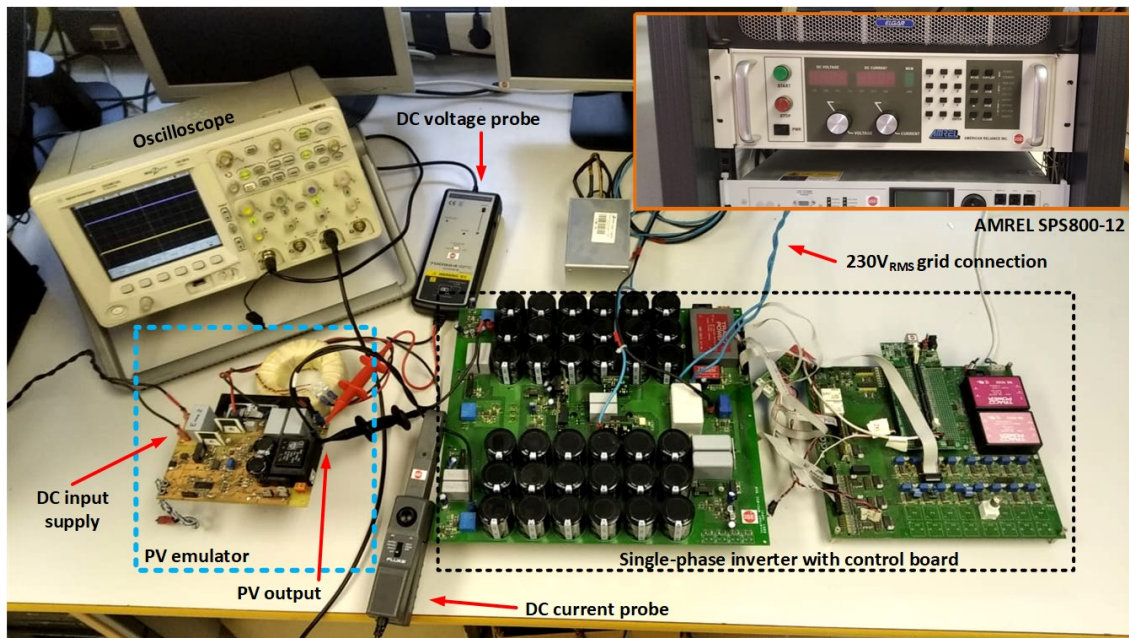


Fig. 8. Experimental setup.

The duration of the programmed irradiance profile is 300 seconds and emulates an incoming shadow. During the first 90 seconds, the irradiance is set to a homogenous level of $1000\text{W}/\text{m}^2$ for all the panels forming the string, and the operating point reaches the MPP at $t \approx 50$ s. At $t = 90$ s the irradiance level of two of the panels starts to fall at the rate of $20\text{ W}/\text{m}^2\text{s}$ until their irradiance level reaches $400\text{W}/\text{m}^2$ at $t = 120$ s. The shadowing process continues with the next block of two panels and so on. When the programmed profile arrives to the end, all the panels in the string are irradiated at $400\text{W}/\text{m}^2$. The irradiance profile is depicted in figure 9.

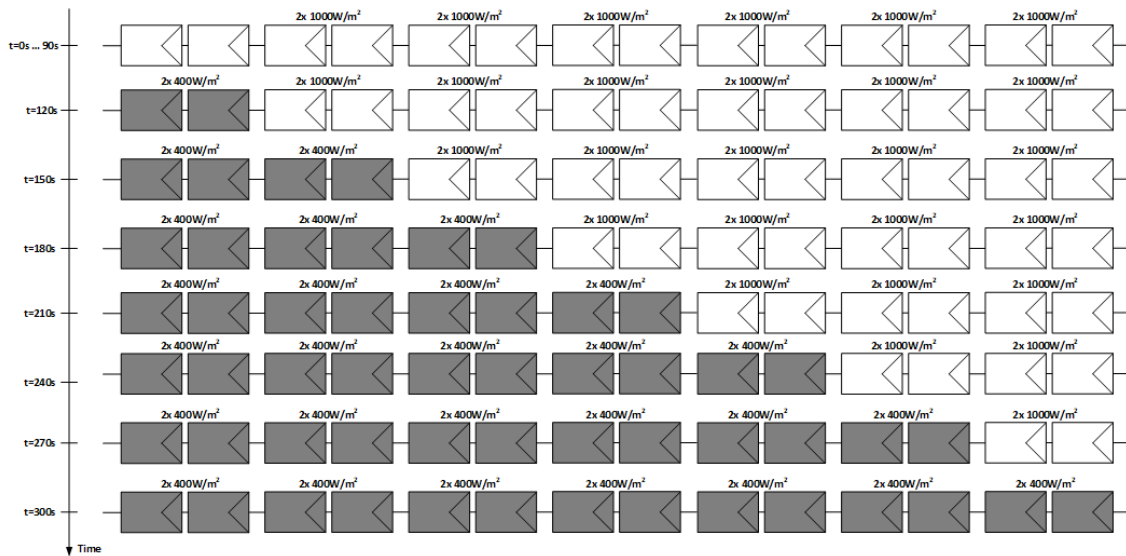


Fig. 9. Irradiance profile for incoming shadow.

When the phenomenon of partial shadowing begins and multiple MPPs appear, the inverter MPPT algorithm fails to track the global MPP. The MPPT algorithm remains latched on a local MPP.

Figure 10 depicts the P-V surface corresponding to the previously described time-varying irradiance profile in the string. In black dots it is represented the evolution of a traditional P&O MPPT algorithm performed by the grid connected inverter.

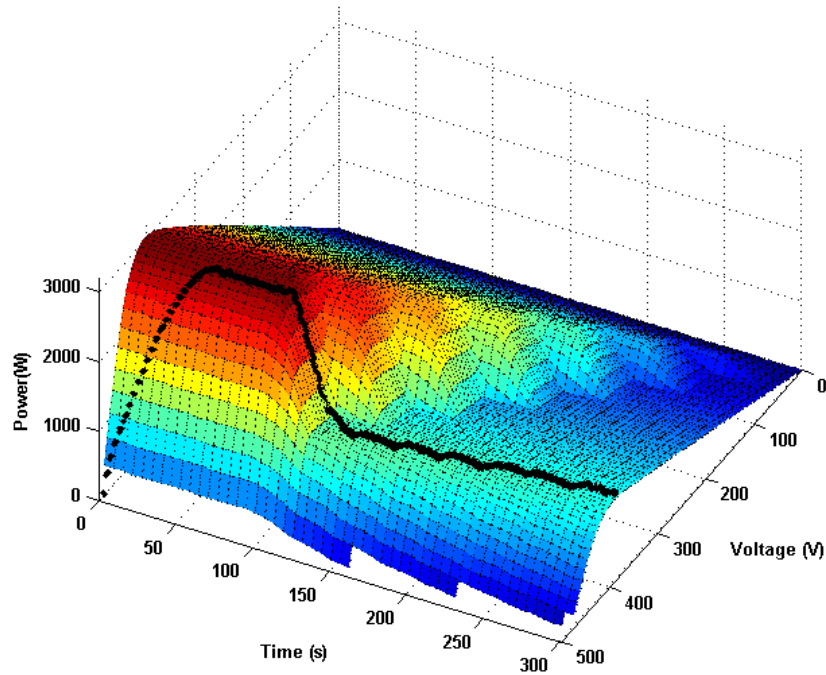


Fig. 10. P-V curves evolution of an MPPT algorithm over a time-varying irradiance profile. Temperature = 25°C.

CONCLUSION

To study the partial shadowing phenomena, it is necessary to provide a power source that emulates the I-V characteristics of a PV string with different irradiance or temperature conditions in the modules, both in steady state and in transient conditions. Besides, it is necessary that the testing conditions can be reproduced easily.

The low computational cost algorithm presented in this paper can emulate the static behaviour of a PV panel string with 7 different groups of PV modules connected in series under different irradiance and temperature conditions.

The algorithm is also capable of emulating a PV string dynamically according to arbitrarily programmed irradiance and temperature time-varying profiles. The update of the string I-V curve interpolation is done on-the-fly to allow testing MPPT algorithms under changing partial shadowing.

The prototype of the PV source emulator has been validated by means of experimental results. It has been demonstrated that the output I-V behaviour fits the chosen manufacturer's model, both under uniform and non-uniform irradiance or temperature conditions. Besides, an MPPT algorithm running on a grid-connected PV inverter has been tested with the emulator, showing that the PV emulator is capable of reproducing transient partial shadowing conditions.

Moreover, the cost of the emulator is around 200 €, easily affordable by institutions for educational and training labs, in contrast with the commercial emulators whose cost is usually over thousands of euros.

REFERENCES

- [1] R. Bradai, R. Boukenoui, A. Kheldoun, H. Salhi, M. Ghanes, J-P. Barbot, A. Mellit, "Experimental assessment of new fast MPPT algorithm for PV systems under non-uniform irradiance conditions", *Applied Energy*, Volume 199, 2017, Pages 416-429, doi. 10.1016/j.apenergy.2017.05.045
- [2] Vitelli, M. "On the necessity of joint adoption of both Distributed Maximum Power Point Tracking and Central Maximum Power Point Tracking in PV systems", *Progress in Photovoltaics: Research and Applications*, 2012. DOI: 10.1002/pip.2256
- [3] Hohm, D. P.; Ropp, M. E. "Comparative study of maximum power point tracking algorithms", *Progress in Photovoltaics: Research and Applications*, 11: 47–62, 2003. DOI: 10.1002/pip.459
- [4] Banu, I.V.; Beniuga, R.; Istrate, M. "Comparative analysis of the perturb-and-observe and incremental conductance MPPT methods," *Advanced Topics in Electrical Engineering (ATEE)*, 2013 8th International Symposium on , vol., no., pp.1,4, 23-25, May 2013. DOI : 10.1109/ATEE.2013.6563483

- [5] Anurag Singh Yadav, V. Mukherjee, "Conventional and advanced PV array configurations to extract maximum power under partial shading conditions: A review", *Renewable Energy*, Volume 178, 2021, Pages 977-1005, <https://doi.org/10.1016/j.renene.2021.06.029>
- [6] Maria Carmela Di Piazza, Gianpaolo Vitale, "Photovoltaic field emulation including dynamic and partial shadow conditions", *Applied Energy*, Volume 87, Issue 3, 2010, Pages 814-823, doi: 10.1016/j.apenergy.2009.09.036.
- [7] Shah, N.; Chudamani, R. "Comparative evaluation of global peak power point tracking techniques for grid-connected PV system operating under partially shaded condition," *Power Electronics (IICPE)*, 2012 IEEE 5th India International Conference on , vol., no., pp.1,6, 6-8, Dec. 2012. DOI: 10.1109/IICPE.2012.6450414
- [8] Orduz, R.; Solórzano, J.; Egido, M. Á.; Román, E. "Analytical study and evaluation results of power optimizers for distributed power conditioning in photovoltaic arrays", *Progress in Photovoltaics: Research and Applications*, 21: 359–373, 2013. DOI: 10.1002/pip.1188
- [9] Sanchis, P.; López, J.; Ursúa, A.; Gubía, E.; Marroyo, L. "On the testing, characterization, and evaluation of PV inverters and dynamic MPPT performance under real varying operating conditions", *Progress in Photovoltaics: Research and Applications*, 15: 541–556, 2007. DOI: 10.1002/pip.763
- [10] Y. Erkaya, P. Moses, I. Flory and S. Marsillac, "Steady-state performance optimization of a 500 kHz photovoltaic module emulator," 2016 IEEE 43rd Photovoltaic Specialists Conference (PVSC), Portland, OR, USA, 2016, pp. 3205-3208, doi: 10.1109/PVSC.2016.7750257.
- [11] R. Ayop and C. W. Tan, "Rapid Prototyping of Photovoltaic Emulator Using Buck Converter Based on Fast Convergence Resistance Feedback Method," in *IEEE*

- Transactions on Power Electronics, vol. 34, no. 9, pp. 8715-8723, Sept. 2019, doi: 10.1109/TPEL.2018.2886927.
- [12] Y. Vagapov and A. Anuchin, "Low-cost photovoltaic emulator for instructional laboratories," 2016 51st International Universities Power Engineering Conference (UPEC), Coimbra, Portugal, 2016, pp. 1-4, doi: 10.1109/UPEC.2016.8114129
- [13] Younghyun Kim, Woojoo Lee, Massoud Pedram, Naehyuck Chang, "Dual-mode power regulator for photovoltaic module emulation, Applied Energy", Volume 101, 2013, Pages 730-739, doi: 10.1016/j.apenergy.2012.07.025
- [14] A.K. Mukerjee, Nivedita Dasgupta, "DC power supply used as photovoltaic simulator for testing MPPT algorithms", Renewable Energy, Volume 32, Issue 4, 2007, Pages 587-592, <https://doi.org/10.1016/j.renene.2006.02.010>
- [15] Akinyele, J. Belikov, and Y. Levron, "Challenges of microgrids in remote communities: A steep model application," Energies, vol. 11, no. 2, p. 432, 2018.)" DOI: 10.3390/en11020432
- [16] González-Medina, R.; Patrao, I.; Garcerá, G.; Figueres, E. "A low-cost photovoltaic emulator for static and dynamic evaluation of photovoltaic power converters and facilities", Progress in Photovoltaics: Research and Applications, 2012. DOI: 10.1002/pip.2243
- [17] Luque A.; Hegedus S. "Handbook of Photovoltaic Science and Engineering", John Wiley & Sons Ltd, 2007. ISBN 9780471491965
- [18] Villalva, M.G.; Gazoli, J.R.; Filho, E.R. "Comprehensive approach to modeling and simulation of photovoltaic arrays", IEEE Transactions on Power Electronics; 24(5): 1198–1208, 2009. DOI: 10.1109/TPEL.2009.2013862
- [19] M. Piliougine, R.A. Guejia-Burbano, G. Petrone, F.J. Sánchez-Pacheco, L. Mora-López, M. Sidrach-de-Cardona, "Parameters extraction of single diode model for

- degraded photovoltaic modules", *Renewable Energy*, Volume 164, 2021, Pages 674-686, <https://doi.org/10.1016/j.renene.2020.09.035>
- [20] Mäki, A.; Valkealahti, S.; Leppäaho, J. "Operation of series-connected silicon-based photovoltaic modules under partial shading conditions", *Progress in Photovoltaics: Research and Applications*; 20:298–309, 2012; DOI: 10.1002/pip.1138
- [21] Kari Lappalainen, Seppo Valkealahti, "Number of maximum power points in photovoltaic arrays during partial shading events by clouds", *Renewable Energy*, Volume 152, 2020, Pages 812-822, <https://doi.org/10.1016/j.renene.2020.01.119>
- [22] Alajmi, B.N.; Ahmed, K.H.; Finney, S.J.; Williams, B.W. "A Maximum Power Point Tracking Technique for Partially Shaded Photovoltaic Systems in Microgrids," *Industrial Electronics, IEEE Transactions on*, vol.60, no.4, pp.1596,1606, April 2013. DOI: 10.1109/TIE.2011.2168796
- [23] Heydari-doostabad, H.; Keypour, R.; Khalghani, M.R.; Khooban, M.H. "A new approach in MPPT for photovoltaic array based on Extremum Seeking Control under uniform and non-uniform irradiances", *Solar Energy*, Volume 94, August 2013, Pages 28-36, ISSN 0038-092X, 2013. DOI: 10.1016/j.solener.2013.04.025
- [24] Juliana E. Gonçalves, Twan van Hooff, Dirk Saelens, "Simulating building integrated photovoltaic facades: Comparison to experimental data and evaluation of modelling complexity", *Applied Energy*, Volume 281, 2021, doi: 10.1016/j.apenergy.2020.116032